Journal of Cellular Biochemistry 103:1886–1894 (2008)

Regulation of *Fgf10* Gene Expression in Murine Mesenchymal Cells

Jyh-Chang Jean, Jining Lü, Martin Joyce-Brady, and Wellington V. Cardoso*

Department of Medicine, the Pulmonary Center, Boston University School of Medicine, Boston, MA, 02118

Abstract *Fgf10* has a prominent role in organogenesis. In the developing lung, Fgf10 is dynamically expressed in the distal mesenchyme from where it diffuses and activates its epithelial receptor, Fgfr2b, to trigger budding. Little is known about how *Fgf10* expression is regulated. Here we have identified a mouse lung-specific mesenchymal cell line, MLg, which expresses endogenous *Fgf10* and responds to known regulators of *Fgf10* in a way that is reminiscent of the early lung. To gain insights into the mechanisms involved in the transcriptional regulation of *Fgf10* in these cells, we have cloned and analyzed approximately a 4.5 kb region of the mouse *Fgf10* promoter. Promoter deletion analysis and Luciferase reporter assays revealed an upstream region of the *Fgf10* promoter with selective enhancer activity in the MLg, but not in the non-lung-derived cell line NIH3T3. Our data suggest that a potential lung mesenchyme-specific enhancer may exist within this region of the *Fgf10* promoter. J. Cell. Biochem. 103: 1886–1894, 2008.

Key words: Fgf10; gene regulation; lung; retinoic acid; MLg cells; enhancer; Tgfb

Fibroblast growth factor 10 (*Fgf10*) regulates cell proliferation, migration, and survival in a variety of biological processes, including embryonic development and tissue repair [Bellusci et al., 1997; Tagashira et al., 1997; Park et al., 1998; Hogan, 1999; Kato and Sekine, 1999; Lebeche et al., 1999; Warburton et al., 2003; Cardoso and Lu, 2006]. Mouse genetic studies have shown that *Fgf10* is required for morphogenesis of organs, such as the lung, limb, thyroid, pancreas, teeth, inner ear, stomach, and the gut [Min et al., 1998; Sekine et al., 1999; Ohuchi et al., 2000].

In the mouse embryo, *Fgf10* is expressed in mesenchymal cells of developing structures in a local and dynamic fashion, and exerts its effect on endodermal-derived epithelial cells, where its high affinity receptor Fgfr2b is present [Bellusci et al., 1997; Park et al., 1998]. Mesenchymal expression of *Fgf10* at prospective sites of budding is critical for patterning, since it appears to induce and direct epithelial buds to proper positions during morphogenesis. Several genes or signaling pathways are known to influence *Fgf10* expression. Sonic hedgehog (Shh) signaling negatively regulates *Fgf10* expression in the lung [Bellusci et al., 1997; Chuang et al., 2003], while some members of the Tbx family of transcription factors (*Tbx4* and *Tbx5*) upregulate *Fgf10* in the developing limb and lung of the mouse and the chick [Ng et al., 2002; Agarwal et al., 2003; Cebra-Thomas et al., 2003; Sakiyama et al., 2003]. Ectopic expression of *Tbx4* induces *Fgf10* expression and bud formation outside the lung field in the foregut of chick embryo [Sakiyama et al., 2003]. However, there is no lung phenotype in *Tbx4* knockout mice, suggesting redundancy of Tbx family members in regulating *Fgf10* expression in the mouse lung mesenchyme.

Differential regulation of *Fgf10* in developing structures has been reported for pathways such as Wnt, Tgf beta (Tgfb), and retinoic acid (RA). For example, increased Wnt canonical signaling by overexpression of *beta-catenin* in the pancreatic epithelium reduces *Fgf10* expression in pancreatic mesenchyme [Heiser et al., 2006]. By contrast, overexpression of *Wnt5a* in the lung epithelium increases *Fgf10* expression in the lung mesenchyme [Li et al.,

Grant sponsor: NIH/NHLBI; Grant number: (PO1) HL47049.

*Correspondence to: Wellington V. Cardoso, MD, PhD, Pulmonary Center, Boston University School of Medicine, 715 Albany Street, R-304, Boston, MA 02118.
E-mail: wcardoso@bu.edu

Received 28 April 2007; Accepted 23 August 2007
DOI 10.1002/jcb.21584

2005]. In the developing prostate, Tgfb1 treatment downregulates *Fgf10* in the ventral mesenchymal pad, but not in the urethra (Tomlinson et al., 2004). We have previously reported a differential requirement of RA for induction of *Fgf10* in different regions of the developing foregut during organogenesis [Desai et al., 2004]. RA antagonist in cultured E8.5 mouse foregut explants abrogates *Fgf10* expression and bud formation in the prospective lung field, but not in other regions such as thyroid and pancreas, which also require Fgf10 for normal development [Desai et al., 2004].

The mechanisms involved in the regulation of murine *Fgf10* gene in lung versus non-lung mesenchymal cells are poorly understood. Currently, there is limited knowledge about mouse-derived cell lines that express endogenous *Fgf10* that could be reliably used to address this problem. Furthermore, although some information on the *Fgf10* promoter is available [Sasak et al., 2002; Ohuchi et al., 2005], it is still largely unknown how different *cis* regulatory elements influence *Fgf10* expression in lung versus non-lung mesenchymal cells.

Here we have identified a mouse lung-specific mesenchymal cell line, MLg, that expresses endogenous *Fgf10* and is able to respond to RA and Tgfb1, known regulators of *Fgf10*, in a way that is reminiscent of what has been described in the early lung. We show that *Fgf10* expression is differentially regulated by RA in MLg cells, when compared to the non-lung-derived NIH3T3 cells. To gain insights into the mechanisms involved in the transcriptional regulation of *Fgf10* in these cells, we have cloned and analyzed approximately a 4.5 kb region of the mouse *Fgf10* promoter. By using promoter deletion analysis and Luciferase reporter assays, we identified an upstream region of *Fgf10* promoter with selective enhancer activity in the MLg, but not in the NIH3T3 cells. Our results suggest that this region could potentially contain sequences that allow *Fgf10* regulation in mesenchymal cells of the lung.

MATERIALS AND METHODS

Northern Blot Analysis

NIH 3T3 cells and Mle cells were maintained in DMEM with 10% fetal calf serum; MLg cells in Eagle's MEM with 10% calf serum. For TGFb treatment, cells were cultured in 1% serum overnight for serum starvation, then treated with TGFb in serum free medium for 6 h. For RA treatment, cells were cultured in medium with 2% serum overnight and treated with RA in medium with 1% serum, and harvested for RNA extraction [Malpel et al., 2000]. After electrophoresis, blotting, and hybridization membranes were exposed to BioMax film (Kodak) and some were re-probed for *Rarb* or beta-actin (Actb).

Northern probes were generated by PCR using the following primers: forward-cluster 1: CACAAAAGAATCTTTATTGTATGGTTC, backward-cluster 1: GGTACCAGGAGGAAACATTGTAATAAT; forward-cluster 2: TGGAAACAAGTGAGCAAGGGCTC, backward-cluster 2: GCGCGATGCCTTTGCTCTGAGCT; forward-Fgf10: TGGAAACAAGTGAGCAAGGGCTC, backward-Fgf10: CCTCTGCGGTTGGCACCTTCTGGTC. The size of the amplicon was 927 bp for cluster 1, 225 bp for cluster 2, and 650 bp for *Fgf10*.

Primer Extension

This was performed as described in Kuang et al. [2006]. The 30-mer complementary primer, 5′-CCTGGAGTCTAAATGTCAGTGCTTTTCAGCCAGA-3′, was selected from the 5′-prime end of a known *Fgf10* EST sequence and radiolabeled using T4 kinase. Labeled primer (10^5 cpm) was precipitated with 100 μg of total RNA, isolated from NIH3T3 or MLg cells or E14 lung, then dissolved in 30 μl of hybridization buffer, denatured and hybridized overnight. Reverse transcription was performed (SuperScript II, Gibco/Invitrogen) at 42°C for 2 h in the presence of 50 μg/ml actinomycin D. The fmol DNA Cycle Sequencing System was selected to generate a sequence marker with the same radiolabeled primer and the 5′-flanking sequence of *Fgf10* as template. tRNA was used as negative control. The cDNA product and the sequencing markers were separated on a polyacrylamide/7 M urea gel.

S1 Nuclease Mapping Analysis

Mapping of the 5′-end of the mouse Fgf10 cDNA onto the gene was performed according to manufacturer's instructions using the S1 nuclease protection assay kit from Ambion (Austin, TX). Poly(A)$^+$ RNA obtained from NIH3T3 cells, 1 or 3 μg, was incubated with a purified ^{32}P-labeled, single-stranded probe encompassing two transcription start sites identified by primer extension (−270 to +134, Fig. 2). After S1 nuclease hydrolysis, protected

fragments were resolved on a 6% acrylamide/7 M urea gel and visualized with autoradiography together with a sequence ladder [Jean et al., 1999].

Plasmid Construction, Cell Cultures, and Transfection Assays

Fgf10-luciferase plasmids were constructed by subcloning genomic sequences into the promoterless pGL3 vector (Promega). Nine promoter constructs were cloned using DNA fragments from −4444, −3531, −2848, −2259, −1038, −588, −149, −6 and +72 to +366 downstream. Promoter activity was assessed in vitro using mouse embryonic NIH3T3 cells, mouse lung epithelial cells (Mle), and mouse lung-derived mesenchymal cells (MLg, ATCC Global Resources; Catalog #CCL-206) [Yoshikura, 1975]. All cells were maintained in culture as described under Northern analysis and transfected by electroporation using 15 μg of plasmid DNA (13 μg *Fgf10*-luciferase, 2 μg of CMV-β-galactosidase) as described previously [Jean et al., 1999, 2006]. Cells were assayed for reporter gene activity 40–48 h after transfection. Each transfection experiment was repeated at least three times. Data were analyzed by Statistical Software package from StatSoft (Tulsa, OK) as described [Jean et al., 2006]. In all of these experiments the negative control was the promoterless-luciferase construct, pGL3-Basic, and the positive control was the SV40 promoter-luciferase construct, pGL3-SV40. The luciferase assay was performed according to the manufacturer's guidelines. Transfection efficiency was normalized by co-transfection with a CMV-β-galactosidase construct as described by Jean et al. [1999, 2006].

RESULTS AND DISCUSSION

Endogenous Fgf10 Is Differentially Regulated by RA and Tgfb in NIH3T3 and MLg Cells

In a screen for mesenchymal cell lines suitable for studies of *Fgf10* gene regulation in vitro, we found that MLg, a fibroblast cell line derived from neonatal mouse lungs, expresses

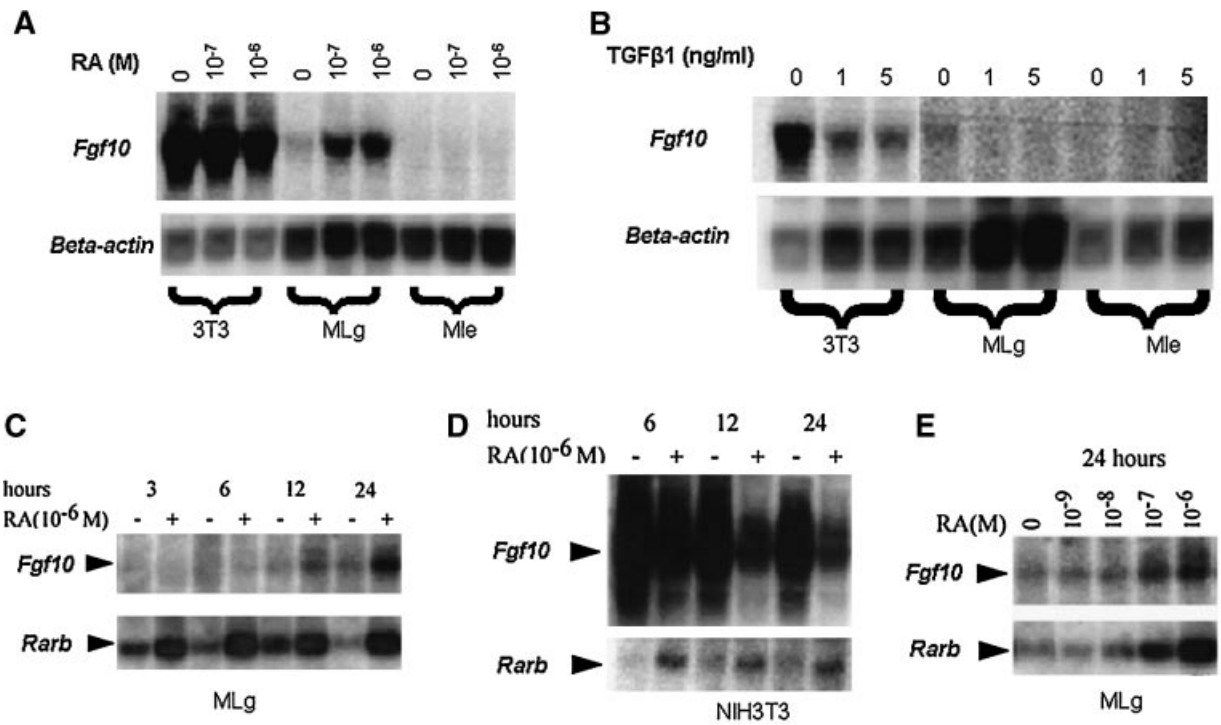

Fig. 1. *Fgf10* expression is differentially regulated by retinoic acid in MLg and NIH3T3 cells. Retinoic acid (RA) treatment downregulated *Fgf10* mRNA expression in NIH3T3 cells, but upregulated *Fgf10* expression in MLg cells (**A**). TGFb downregulates *Fgf10* expression in both MLg cells and NIH3T3 cells (Beer et al., 1997). Mle cells in (A) and (**B**) serve as a negative control for *Fgf10* mRNA expression. Induction of *Fgf10* mRNA is evident within 12 and 24 h after RA incubation (**C**), even though *Rarb* induction is detectable within 3 h of treatment in MLg cells changes in *Fgf10* expression was evident 12 h after RA treatment. Changes in expression of both *Fgf10* and *Rarb* mRNAs are detectable within 6 h of RA treatment in NIH3T3 cells (**D**). RA at 10^{-7} M upregulates *Fgf10* and *Rarb* mRNAs in MLg cells (**E**).

endogenous *Fgf10*. To test if regulation of *Fgf10* expression could be studied in these cells, we treated non-confluent MLg cells with RA or Tgfb1, two molecules known to modulate *Fgf10* gene expression in other systems [Chuang et al., 2003; Tomlinson et al., 2004; Desai et al., 2004]. Results were compared with those from the non-lung-specific NIH3T3 cells treated similarly with RA or Tgfb1.

We found that RA increased *Fgf10* mRNA expression in MLg cells (Fig. 1A), and this induction occurred at a physiological level of RA (10^{-7} M, as shown in Fig. 1E). In contrast, RA treatment decreased *Fgf10* mRNA expression in NIH3T3 cells in a dose-dependent fashion (Fig. 1A). Mle epithelial cells do not express *Fgf10* mRNA, and serve as a negative control in Figure 1A and B. *Rarb*, one of the receptors for RA, is also known to be one of the earliest RA transcription targets, thus serving as a reporter of the RA signaling activation [Harnish et al., 1990]. As shown in Figure 1C–E, *Rarb* expression was upregulated in response to RA treatment in MLg, NIH3T3, and Mle cells.

Interestingly, RA-induced upregulation of *Fgf10* mRNA in MLg cells was only evident 12 h after treatment (Fig. 1C), whereas RA-induced downregulation of *Fgf10* mRNA in NIH3T3 was detectable within 6 h of treatment (Fig. 1D). We also treated these cells with recombinant Tgfb1, which has strong inhibitory activity suppressing *Fgf10* expression in cells and organ cultures [Lebeche et al., 1999]. In contrast to RA, Tgfb1 consistently inhibited *Fgf10* expression in both cell types (Fig. 1B). The regulation of Fgf10 by RA in MLg cells differed from NIH3T3, and appeared to be similar to those reported in the developing lung mesenchyme at early stages [Serra et al., 1994; Desai et al., 2004].

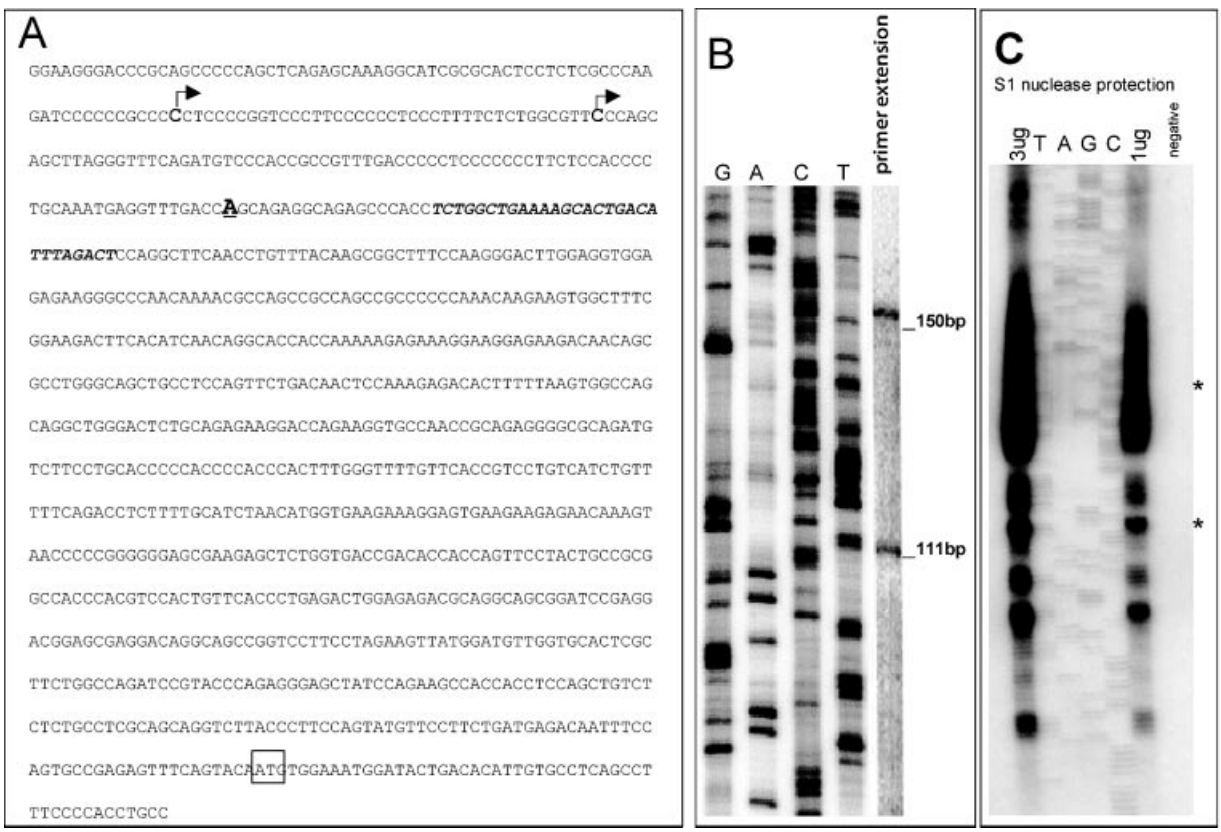

Fig. 2. Mouse Fgf10 gene transcription start sites. Partial promoter sequences of mouse *Fgf10* is shown in panel (**A**), and the longest *Fgf10* EST ending at 757 bps upstream of the ATG is denoted by the underlined A. The 30-mer selected for primer extension is italicized in bold, and the two transcription start sites mapped by primer extension (**B**, E14.5 lung) are located 819 and 858 bps upstream of ATG within a GC rich region. S1 nuclease protection assay was used to map transcription start sites of *Fgf10* in NIH3T3 cells (**C**). The two transcription start sites (asterisk) mapped by primer extension overlap with several clusters of transcription start sites mapped to the same region by S1 nuclease protection assay.

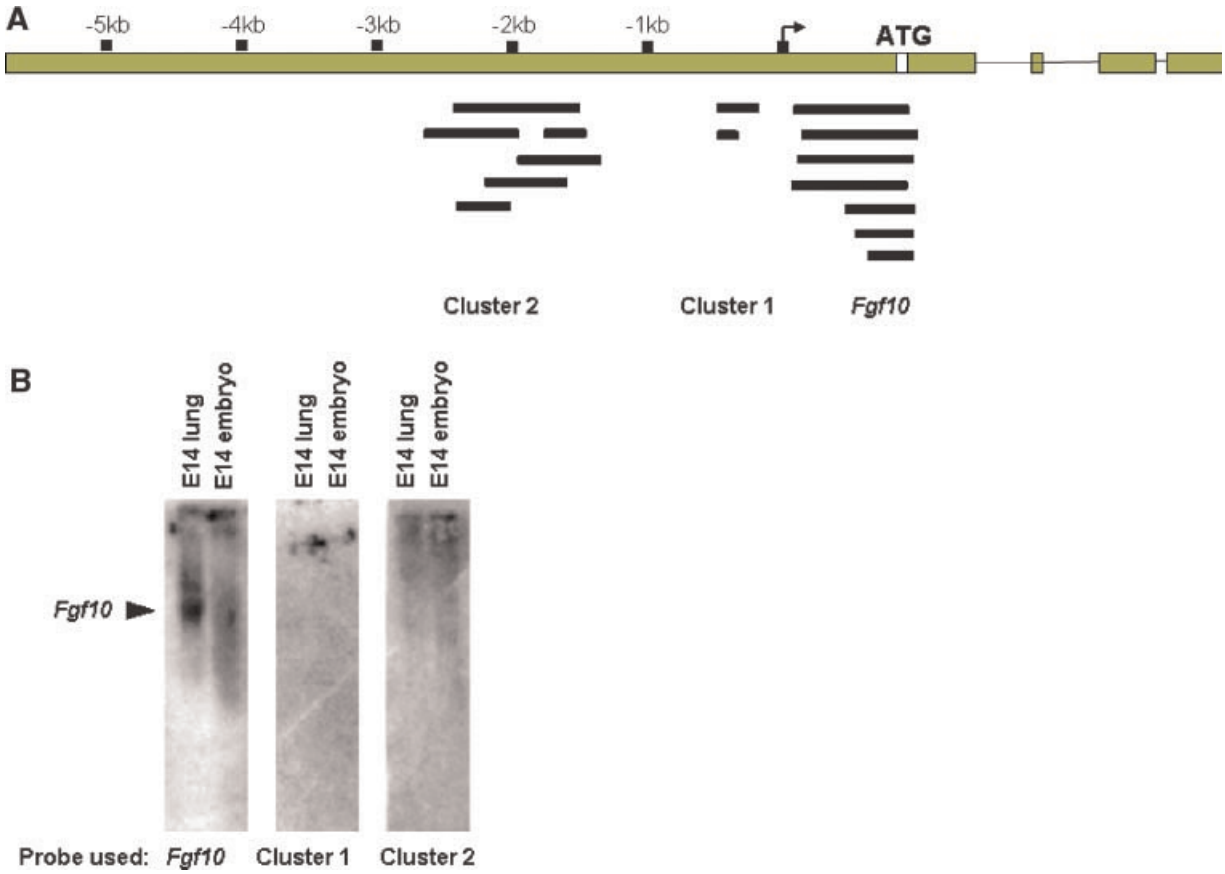

Fig. 3. Exclusion of two clusters of EST sequences located upstream of the *Fgf10* transcription start sites from *Fgf10* mRNA. The schematic in panel (**A**) shows two clusters of EST sequences identified by searching the NCBI mouse EST database and located just upstream of the mapped transcription start sites. These EST sequences included transcripts from both the plus and the minus strands. To determine if these were upstream exons of *Fgf10* mRNA, not detected by our primer extension, probes from *Fgf10* cDNA and the two upstream EST regions were used in a Northern analysis with total RNA derived from E14 embryonic lung or E14 whole embryo. Panel (**B**) shows that a hybridization signal was only detected using probe from *Fgf10* cDNA, suggesting that the upstream EST sequences are not part of *Fgf10* mRNA. [Color figure can be viewed in the online issue, which is available at www.interscience.wiley.com.]

Fig. 4. A potential lung mesenchymal cell-specific enhancer in the mouse *Fgf10* promoter. **A**: A schematic of the nine-cloned reporter constructs (''i'' through ''a'') covering about 4.5 kb upstream and downstream of the transcription start site (tss). **B**: Their activities in MLg cells (mouse lung mesenchymal cell line) and NIH3T3 cells in reporter constructs with sequences downstream of tss (''i'' and ''h'') have no more activity than the promoter-less basic reporter control. Reporter activities are significantly increased with additional sequences upstream of the tss (''g'' through ''a'') in both cell lines suggesting promoter activity in the region surrounding our mapped tss (asterisk and cross denoted significant activity of reporter constructs compared to the basic construct with $P < 0.05$). Reporter activity increased significantly and successively from constructs ''c'' to ''b'' to ''a'' in MLg cells ($P < 0.05$, double cross), but not in NIH3T3 cells. Constructs ''a'' and ''b'' include about 1.5 kb of additional upstream sequences (designated as fragment ''T'') compared to the other constructs suggesting the presence of lung-specific enhancer activity within this region. **C**: Potential lung mesenchymal cell enhancer activities are located in the 5′ and the 3′ regions of fragment ''T''. A schematic of the four luciferase promoter reporters cloned for the intact fragment ''T'' as well as internal segments X, Y, and Z from fragment ''T'', together with their activities analyzed by transient transfection are shown for MLg cells and NIH3T3 cells. Reporter gene activity analyzed significantly above that of the SV40 promoter control (asterisks, $P < 0.05$) was detected in the intact fragment ''T'', and in segments X and Y, but not Z specifically in MLg cells. None of these constructs increased reporter activity in NIH3T3 cells above that of the SV40 promoter control. Lung mesenchymal cell-specific enhancer activities reside in both the 5′ and the 3′ regions of fragment ''T''. [Color figure can be viewed in the online issue, which is available at www.interscience.wiley.com.]

Characterization of the Mouse Fgf10 Promoter

To better understand the basis for the differential regulation of the *Fgf10* gene in lung versus non-lung mesenchymal-derived cells, we cloned and analyzed the murine Fgf10 promoter in classical Luciferase reporter assays.

First we characterized the transcription start site of *Fgf10* gene. Northern blot analysis

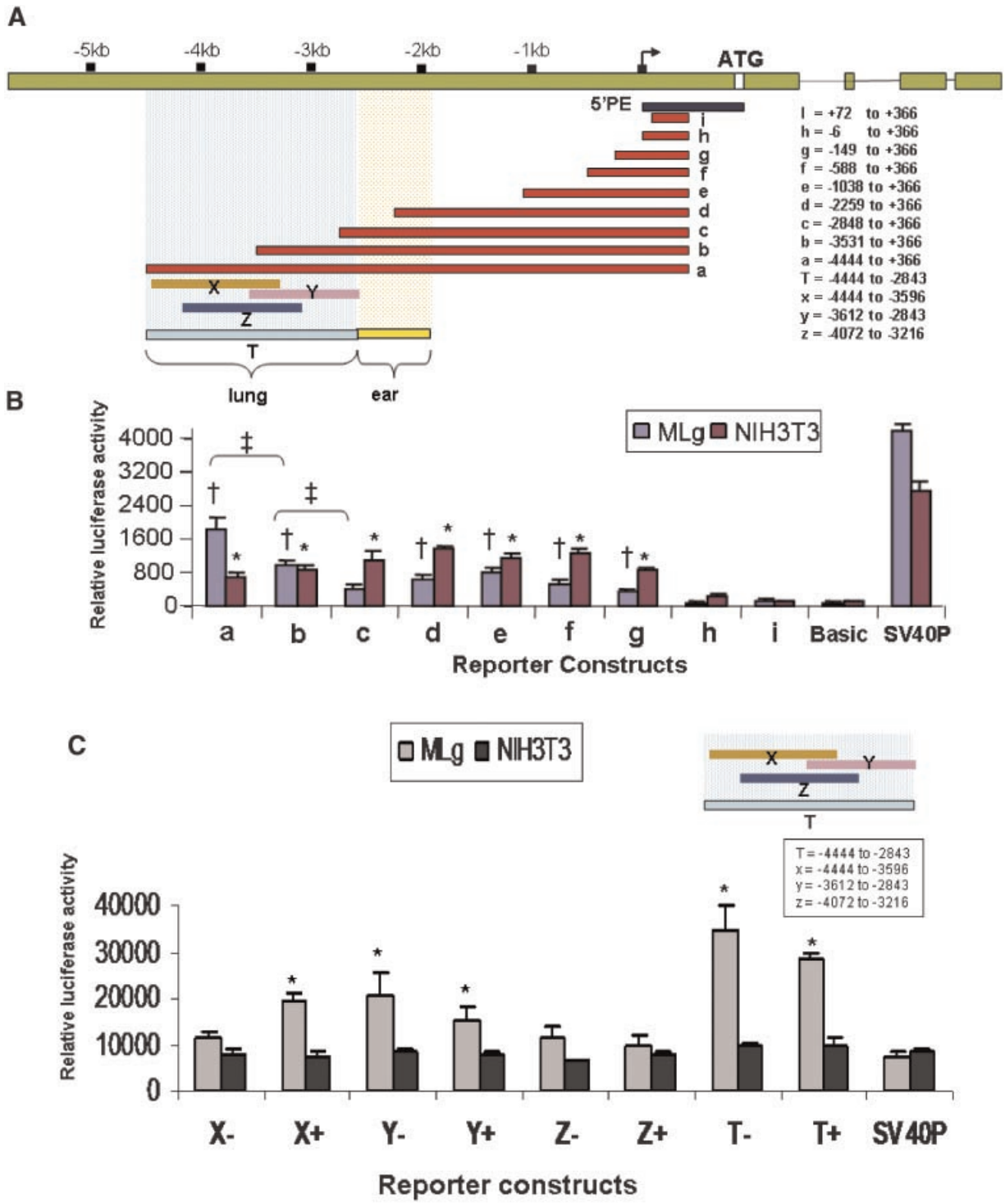

Fig. 4.

revealed a 4.5 kb *Fgf10* mRNA that was abundantly expressed in whole embryos and embryonic lung [Beer et al., 1997]. A 4.3 kb *Fgf10* transcript was assembled *in silico* by combining the longest cDNA with a poly(A) tail in GenBank (BC048229.1) and the EST sequence (BB660212) from embryonic day 13 lungs containing the most 5′ sequences. This transcript ends 757 bp upstream of the ATG (boxed in Fig. 2A) of *Fgf10*, and its size suggests proximity of the 5′-end to the transcription start site (underlined and bolded Adenine residue also in Fig. 2A).

We performed primer extension analysis using a 30-mer oligonucleotide (bold italic in Fig. 2A) located at the 5′-end of the longest transcript. This generated two specific upstream primer extension products of 111 bp and 150 bp (Fig. 2A,B). Based on the overall size of the *Fgf10* mRNA from Northern analysis, it is likely that these represented two transcription start sites for the mouse *Fgf10* gene. No TATA box was identified for both transcription start site and it is typical that a TATA-less promoter has multiple transcription start sites. The similar intensity of each primer extension product suggests the lack of any preferential usage. To further confirm our primer extension results, we used S1 nuclease protection assay to map the transcription initiation sites of *Fgf10* in NIH3T3 cells. Figure 2C shows that protected DNA fragments are only detected in samples with RNA from NIH3T3 cells, but not from negative control tRNA. We found that the two transcription start sites (asterisk) mapped by primer extension are in the same region where several clusters of transcription start sites were also identified by S1 nuclease protection assay. This suggests that these original transcription start sites are accurate sites for Fgf10 gene expression in both embryonic lung and in NIH3T3 cells. More start sites were identified by S1 nuclease protection as this assay is more sensitive than primer extension.

We then searched for potential transcripts generated from this region by examining EST sequences homologous to the 4 kb genomic DNA sequence extending 1 kb downstream and 3 kb upstream of the putative transcription start sites. We found three clusters of EST sequences that align to this region (Fig. 3A). One cluster corresponded to 5′ sequences of *Fgf10*, but the two other clusters, located further upstream, lacked any overlap with the longest *Fgf10* transcript, and contained ESTs transcribed from both the sense and the antisense strands. To determine if the EST sequences from these two upstream clusters could represent additional 5′ exons of mouse *Fgf10* mRNA transcripts, we generated probes from each region for Northern blot analysis. Using a probe derived from the 5′ sequence of *Fgf10* and total RNA samples derived from E14 embryonic lung and E14 embryos, a stage when *Fgf10* is abundantly expressed, we detected a strong and a weak 4.5 kb signal from the lung and the whole embryo, respectively (see probe used: Fgf10 in Fig. 3B). However, no signal was detected in any sample if the probes were derived from either of the two upstream clusters (Cluster 1 and Cluster 2 in Fig. 3B). These data suggest that EST sequences from the two upstream clusters are not part of *Fgf10* mRNA. We cannot exclude the possibility that very low abundance *Fgf10* mRNA transcripts include sequences from these regions, but our data strongly suggest that the primary species of *Fgf10* mRNA are transcribed from the transcription start sites that we mapped by primer extension.

Characterization of a Promoter Region With Specific Enhancer Activity in the Lung Mesenchymal Cell Line

We then examined whether the DNA sequences around the transcription start sites of mouse *Fgf10* exhibited promoter activity in MLg and NIH3T3 cells. Nine DNA fragments were cloned into the promoter-less luciferase reporter construct (pGL3-Basic) including sequences both upstream and downstream of the *Fgf10* transcription start sites (see constructs a–i in Fig. 4A). We defined the 3′ transcription start site as +1, and the designated regions in all reporter constructs refer to this start site. These constructs were examined for reporter gene activity after transient transfection into mesenchymal cells derived from mouse lung, MLg, or from whole mouse embryo, NIH3T3 (Fig. 4B). Neither constructs "i" nor "h" produced any increased luciferase activity in either cell line compared to that of the pGL3-Basic vector control, suggesting an absence of promoter activity in these two fragments. These results are consistent with our transcription start site data as both are located downstream of our putative *Fgf10* transcription start sites. Thereafter, promoter activities increased above the pGL3-Basic vector control for all other constructs ("g" through "a") using the

core promoter region and additional upstream regions of *Fgf10* in both MLg and NIH3T3 cells. These data support the accuracy of the core promoter region that we have identified.

In general, we detected relatively higher reporter gene activities in NIH3T3 cells compared to that of MLg cells for most of our promoter constructs which may reflect the higher level of endogenous *Fgf10* transcript expression in NIH3T3 cells. The trend was most evident for constructs "g" through "c", but then diverged in reporter constructs "b" and "a", which showed a progressive increase in activity with the addition of more 5′ prime sequences in MLg cells as shown in Figure 4B. Reporter construct "b" had a similar level of activity in MLg and NIH3T3 cells, but reporter construct "a" had much higher activity in MLg cells than in NIH3T3 cells. These data suggest the presence of a MLg cell-specific enhancer activity in the 5′-region of reporter constructs "b" and "a" (hereafter denoted region "T"), which is absent from the more proximal reporter constructs. Interestingly, an *Fgf10* enhancer region specific for the inner ear has recently been described [Ohuchi et al., 2005], and is positioned just downstream of our putative lung-specific enhancer.

To examine this in detail, we cloned region "T", a 1 kb fragment of DNA wherein the MLg enhancer activity resides, upstream of the pGL3-SV40 promoter vector in both orientations, and analyzed these constructs by transient transfection assays in MLg and NIH3T3 cells (Fig. 4C). Construct "T" significantly increased reporter gene activity in MLg cells by threefold over that of the SV40 promoter vector alone in an orientation-independent fashion characteristic of an enhancer element. No such increase in activity was seen in NIH3T3 cells suggesting that this segment of DNA is selectively active in MLg cells.

We then divided construct "T" into three overlapping fragments spanning sequences in the 5′-end (X), the 3′-end (Y), and the center (Z) of the intact 1.5 kB region. These three fragments were cloned upstream of the pGL3-SV40 promoter vector in both orientations and were again examined for enhancer activity (Fig. 4C). Construct Y exhibited clear orientation-independent enhancer activity in MLg cells beyond that of the SV40 promoter vector alone, construct X showed orientation-specific activity and construct Z exhibited no increase in activity at all above that of the SV40 promoter alone. These data suggest that the MLg-selective enhancer activity resides in the 5′-end of construct X, and the 3′-end of construct Y within the intact 1.5 kB enhancer region, thereby localizing potential cis-elements within the enhancer. Again none of these constructs increased reporter activity in NIH3T3 cells over that of the SV40 promoter alone further supporting specificity of the MLg cell enhancer activity.

Concluding Remarks

In summary, we provide evidence for differential regulation of *Fgf10* mRNA expression in two types of mesenchymal cells. In certain instances, regulation occurs in the same fashion (as for Tgfb1), but in others, such as RA, both the kinetics and the direction of the response differ in MLg cells compared to NIH3T3 cells. The exact mechanisms involved in this differential response to RA are still unclear and will require further investigation. This difference in RA responsiveness may be related to cell-specific transcription or post-transcriptional mechanisms that regulate mouse *Fgf10* mRNA expression. In our Fgf10 promoter analysis, we identified an enhancer residing in the 5′-end of our construct selectively activating *Fgf10* expression in the lung-derived mesenchymal cell line MLg, but not in NIH3T3 cells. Our data suggest that this region may represent a lung-specific enhancer.

Our mapping of the transcription start sites, localization of a lung mesenchymal cell-specific enhancer and identification of differential regulation of mouse *Fgf10* in lung mesenchymal cells establishes a foundation for future studies using reporter constructs in transgenic mice.

REFERENCES

Agarwal P, Wylie JN, Galceran J, Arkhitko O, Li C, Deng C, Grosschedl R, Bruneau BG. 2003. Tbx5 is essential for forelimb bud initiation following patterning of the limb field in the mouse embryo. Development 130:623–633.

Beer HD, Florence C, Dammeier J, McGuire L, Werner S, Duan DR. 1997. Mouse fibroblast growth factor 10: cDNA cloning, protein characterization, and regulation of mRNA expression. Oncogene 15:2211–2218.

Bellusci S, Grindley J, Emoto H, Itoh N, Hogan BL. 1997. Fibroblast growth factor 10 (FGF10) and branching morphogenesis in the embryonic mouse lung. Development 124:4867–4878.

Cardoso WV, Lu J. 2006. Regulation of early lung morphogenesis: questions, facts and controversies. Development 133:1611–1624.

Cebra-Thomas JA, Bromer J, Gardner R, Lam GK, Sheipe H, Gilbert SF. 2003. T-box gene products are required for mesenchymal induction of epithelial branching in the embryonic mouse lung. Dev Dyn 226:82–90.

Chuang PT, Kawcak T, McMahon AP. 2003. Feedback control of mammalian Hedgehog signaling by the Hedgehog-binding protein, Hip1, modulates Fgf signaling during branching morphogenesis of the lung. Genes Dev 17:342–347.

Desai TJ, Malpel S, Flentke GR, Smith SM, Cardoso WV. 2004d. Retinoic acid selectively regulates Fgf10 expression and maintains cell identity in the prospective lung field of the developing foregut. Dev Biol 273:402–415.

Harnish DC, Barua AB, Soprano KJ, Soprano DR. 1990. Induction of beta-retinoic acid receptor mRNA by teratogenic doses of retinoids in murine fetuses. Differentiation 45:103–108.

Heiser PW, Lau J, Taketo MM, Herrera PL, Hebrok M. 2006. Stabilization of beta-catenin impacts pancreas growth. Development 133:2023–2032.

Hogan BL. 1999. Morphogenesis. Cell 96:225–233.

Jean JC, Oakes SM, Joyce-Brady M. 1999. The Bax inhibitor-1 gene is differentially regulated in adult testis and developing lung by two alternative TATA-less promoters. Genomics 57:201–208.

Jean JC, Rich CB, Joyce-Brady M. 2006. Hypoxia results in an HIF-1-dependent induction of brain-specific aldolase C in lung epithelial cells. Am J Physiol Lung Cell Mol Physiol 291:L950–L956.

Kato S, Sekine K. 1999. FGF-FGFR signaling in vertebrate organogenesis. Cell Mol Biol (Noisy-le-grand) 45:631–638.

Kuang PP, Joyce-Brady M, Zhang XH, Jean JC, Goldstein RH. 2006. Fibulin-5 gene expression in human lung fibroblasts is regulated by TGF-beta and phosphatidylinositol 3-kinase activity. Am J Physiol Cell Physiol 291: C1412–C1421.

Lebeche D, Malpel S, Cardoso WV. 1999. Fibroblast growth factor interactions in the developing lung. Mech Dev 86: 125–136.

Li C, Hu L, Xiao J, Chen H, Li JT, Bellusci S, Delanghe S, Minoo P. 2005. Wnt5a regulates Shh and Fgf10 signaling during lung development. Dev Biol 287:86–97.

Malpel S, Mendelsohn C, Cardoso WV. 2000. Regulation of retinoic acid signaling during lung morphogenesis. Development 127:3057–3067.

Min H, Danilenko DM, Scully SA, Bolon B, Ring BD, Tarpley JE, DeRose M, Simonet WS. 1998. Fgf-10 is required for both limb and lung development and exhibits striking functional similarity to Drosophila branchless. Genes Dev 12:3156–3161.

Ng JK, Kawakami Y, Buscher D, Raya A, Itoh T, Koth CM, Rodriguez EC, Rodriguez-Leon J, Garrity DM, Fishman MC, Izpisua Belmonte JC. 2002. The limb identity gene Tbx5 promotes limb initiation by interacting with Wnt2b and Fgf10. Development 129:5161–5170.

Ohuchi H, Hori Y, Yamasaki M, Harada H, Sekine K, Kato S, Itoh N. 2000. FGF10 acts as a major ligand for FGF receptor 2 IIIb in mouse multi-organ development. Biochem Biophys Res Commun 277:643–649.

Ohuchi H, Yasue A, Ono K, Sasaoka S, Tomonari S, Takagi A, Itakura M, Moriyama K, Noji S, Nohno T. 2005. Identification of cis-element regulating expression of the mouse Fgf10 gene during inner ear development. Dev Dyn 233:177–187.

Park WY, Miranda B, Lebeche D, Hashimoto G, Cardoso WV. 1998. FGF-10 is a chemotactic factor for distal epithelial buds during lung development. Dev Biol 201: 125–134.

Sakiyama J, Yamagishi A, Kuroiwa A. 2003. Tbx4-Fgf10 system controls lung bud formation during chicken embryonic development. Development 130:1225–1234.

Sasak H, Yamaoka T, Ohuchi H, Yasue A, Nohno T, Kawano H, Kato S, Itakura M, Nagayama M, Noji S. 2002. Identification of cis-elements regulating expression of Fgf10 during limb development. Int J Dev Biol 46:963–967.

Sekine K, Ohuchi H, Fujiwara M, Yamasaki M, Yoshizawa T, Sato T, Yagishita N, Matsui D, Koga Y, Itoh N, Kato S. 1999. Fgf10 is essential for limb and lung formation. Nat Genet 21:138–141.

Serra R, Pelton RW, Moses HL. 1994. TGF beta 1 inhibits branching morphogenesis and N-myc expression in lung bud organ cultures. Development 120:2153–2161.

Tagashira S, Harada H, Katsumata T, Itoh N, Nakatsuka M. 1997. Cloning of mouse FGF10 and up-regulation of its gene expression during wound healing. Gene 197: 399–404.

Tomlinson DC, Grindley JC, Thomson AA. 2004. Regulation of Fgf10 gene expression in the prostate: Identification of transforming growth factor-beta1 and promoter elements. Endocrinology 145:1988–1995.

Warburton D, Bellusci S, Del Moral PM, Kaartinen V, Lee M, Tefft D, Shi W. 2003. Growth factor signaling in lung morphogenetic centers: Automaticity, stereotypy and symmetry. Respir Res 4:5.

Yoshikura H. 1975. Clonal variation of the mouse cells in the endogenous C-type virus induction by 5-iodo-2′-deoxyuridine. J Gen Virol 28:179–184.